Chapter 5 Photodetection Application of MoS_2 Nanostructures

5.1 Introduction

The electromagnetic signal (light) possessing spectral wavelength from X-ray to infrared region; carries vital information. Among electronic and optoelectronic devices, photodetectors are becoming a key component of optoelectronic technology due to their wide range of applications such as imaging, remote sensing, spectroscopy, robotics, night vision, security, motion detection and digital communication. The ultra-fast detectors are required in telecommunication applications, while relatively slow speed is required to have good sensitivity for the detection of low intensity lights in imaging system. In photodetectors, incident photons (light) are converted into electrical signals [92]. The performance of photodetectors depends on different factors like light absorption, electron-hole pair generation, separation of the charge carrier, and the charge transport [6]. Different kinds of semiconducting materials are used for photodetection applications based on their stability, responsivity and efficiency. Recently, 2D transition metal dichalcogenides (TMDs) have attracted huge attention of the scientific community for optoelectronics application due to their unique properties such as tunable bandgaps, strong interaction with light and the presence of weak interlayer bonding [6, 11, 13]. TMDs are earth-abundant and have emerged as 2D materials of choice due to multiple advantages such as their low-cost production, easy synthesis and they can be easily transferred on a required substrate with precise thickness [33, 183]. The 2D-TMDs have enormous advantages in various photonic and optoelectronic applications due to their energy bandgaps covering the visible and near-infrared spectral region, which is suitable for ultra-broadband photodetectors. The most interesting properties in TMDs structures are layer dependent bandgaps and quantum efficiency.

The presence of direct electronic transitions in monolayer MoS_2 increases the probability for excitons (electron-hole pairs) generation [184,185]. Monolayer MoS_2 possess high carrier mobility and optical transparency compared to conventional semiconductors, making it suitable for developing ultra-broadband photodetectors for use in different areas such as surveillance and sensor for real-life applications [93, 186]. Photoconduction based MoS_2 photodetector devices can be made in two different ways- p-n junction device and metal-semiconductor-metal (MSM) device. In literature, a wide range of studies on MoS_2 based photodetectors were performed. Midya *et al*. observed the responsivity of 0.045 A W^{-1} for the MoS_2/Si photodiode under the illumination of visible Laser (514 nm) with power density of 3 mW cm^{-2} at applied bias of -2V [24]. Shin *et. al.* also reported the vertical p-type Si/n-type MoS_2 heterojunction photodetector prepared by mechanically exfoliated n-type MoS_2 flakes with photoresponsivity of 76 A W^{-1} under excitation of 12 nW at reverse voltage of 5V [187]. Mukherjee *et. al.* demonstrated MoS_2 nanocrystals of varying dimensions with maximum photoresponsivity of the device around 0.133 A W^{-1} at -2V under 514 nm laser excitation for 18 nm MoS_2 nanocrystal [188]. Dhyani and Das reported the few-layer MoS_2 for photodetection using Si/MoS_2 (p-n) heterojunction devices [61]. They observed photoresponsivity of ~ 8.75 A W^{-1} for p-n junction device and attributed the higher photoresponsivity to the presence of additional charge carriers in p-type Si substrate. Wang *et al.* reported the synthesis of few-layer V-type MoS_2 over Si substrate via sputtering technique and observed the photoresponsivity of the device ~ 0.3 A W^{-1} under the 808 nm laser illumination [189]. In the present work, we have demonstrated photoconduction behaviour of CVD grown MoS_2 nanostructures in p-n junction configuration as shown in **Figure 5.1**. In the following section, we will discuss the photodetection applications of horizontally grown interconnected network of few-layer MoS_2 and vertically oriented few-layer MoS_2 on p-type Si substrate.

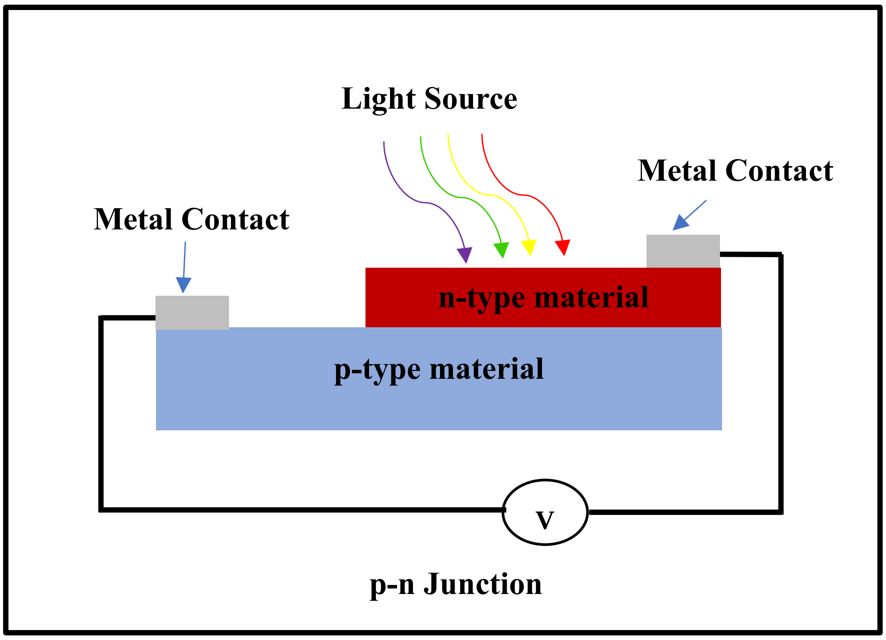

Figure 5.1 *Schematic representation of p-n junction-based photodetector.*

5.2 Results and Discussion

5.2.1 Photodetection Behaviour of Horizontally Grown Interconnected Network of Few-Layer MoS_2

We have grown horizontal interconnected network of few-layer MoS_2 over p-type Si substrate and studied its morphology and semiconducting properties for photodetection application. In the following section, we discuss the photodetection performance of few-layer MoS_2 /Si heterojunction in detail.

5.2.1.1 Characterization of Horizontally Grown Interconnected Few-Layer MoS_2

The surface morphology of the prepared horizontally grown few-layer MoS_2 over Si substrate was characterized by scanning electron microscope (SEM). **Figure 5.2 (a)** shows the SEM image of few-layer MoS_2 film, indicating their large area growth. It shows the interconnected network of few-layer MoS_2 of size around 200-300 nm. The AFM image of this sample is shown in **Figure 5.2 (b)**, indicating the lateral dimensions in the same range and the corresponding thicknesses is found around 4 nm for few-layer MoS_2, as shown in **Figure 5.2 (c)**. It indicates the presence of five to six layers in few-layer MoS_2 film. The variation in height profile (around 1 nm) for AFM image of a few-layer MoS_2 suggests the presence of surface roughness in prepared few-layer MoS_2 film, which facilitates the availability of higher surface area in a given length scale. Vibrational characteristics of few-layer MoS_2 film over Si substrate have been analyzed using Raman spectroscopy. The Raman spectrum of the few-layer MoS_2 is shown in **Figure 5.2 (d)**.

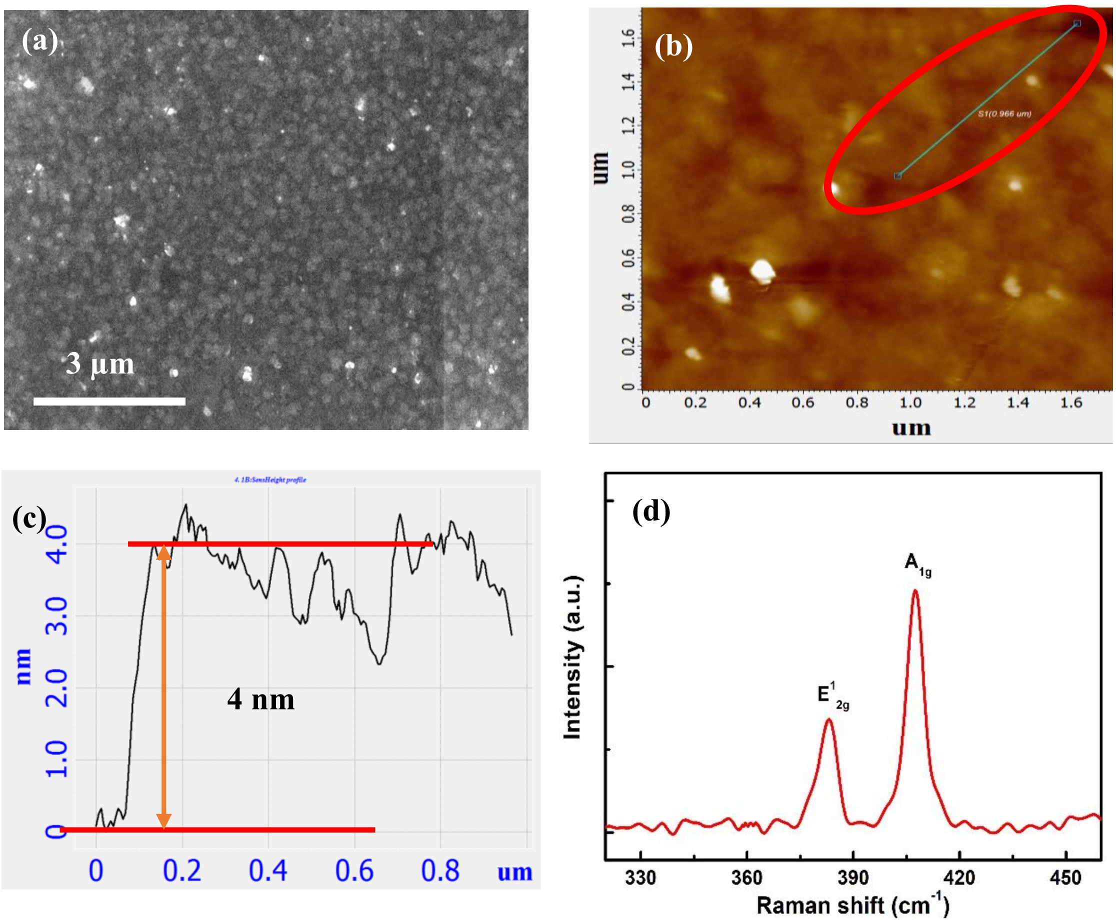

Figure 5.2 *(a) SEM image (b) AFM image (c) Corresponding height profile and (d) Raman spectrum of interconnected network of few-layer MoS_2 over Si substrate.*

The two characteristics peaks of MoS_2 E^1_{2g} (in-plane vibrations) and A_{1g} (out-of-plane vibrations) are observed around 383.2 and 407.4 cm^{-1}, respectively. The presence of E^1_{2g} and A_{1g} modes indicates the formation of the 2H phase few-layer forms of MoS_2. The separation between these two peaks is found around 24.2 cm^{-1}, which indicates the presence of five to six layers in few-layer MoS_2 film as per literature reports [190]. The number of layers observed in Raman study matches with AFM study.

5.2.1.2 Photoresponse of Few-Layer MoS_2/Si Heterojunction

In order to examine the semiconducting nature and suitability of few-layer MoS_2 for photodetection, we performed the PL study, as shown in **Figure 5.3 (a)**. The PL spectrum of few-layer MoS_2 clearly indicates a peak around 683 nm, corresponding to the direct A excitonic transition and a hump around 635 nm due to direct B excitonic transition. It suggests that few-layer MoS_2 contains a direct bandgap of 1.81 eV [6, 191]. The presence of A and B excitonic transitions in interconnected network of few-layer MoS_2 indicates that it can be used for photodetection application. The CVD grown MoS_2 is found usually n-type in nature and it makes good contact with the Si substrate [96]. The photodetection behaviour of n-type interconnected network of few-layer MoS_2/p-type Si heterojunction has been studied in p-n junction configuration, as shown schematically in **Figure 5.1**. The photocurrent has been measured under white light illumination (neon lamp source) at low power densities of 0.05 and 0.15 mW cm^{-2}. **Figure 5.3 (b)** shows the dark current of the heterojunction photodetector. We observe an asymmetry in the I-V characteristics that represents the formation of a good junction between the n-type few-layer MoS_2 and p-type Si substrate. In order to examine the diode characteristics of our fabricated few-layer MoS_2/Si heterojunction, we have calculated the ideality factor (η) from the semi-log $I - V$ curve in the forward bias direction. The ideality factor (η) is given by [186] -

$$\eta = \frac{q}{k_b T}\left(\frac{\partial V}{\partial lnI}\right) \quad (5.1)$$

where k_b, T and q represent Boltzmann's constant, temperature and electronic charge, respectively. It expresses how closely the diode follows the ideal diode equation and for ideal diode its value is expected to be around 1. However, the higher value of the ideality factor represent the recombination and charge trapping in different parts of the device. We have found the value of ideality factor for this heterojunction around 2.74 using **equation 5.1**, which is higher than ideal diode value of 1, suggesting the presence of some defects or impurities at the junction resulting in recombination current. **Figure 5.3 (c)** shows the response of photodetection property of interconnected network of few-layer MoS_2/Si heterojunction under dark and illumination conditions. It indicates that upon white light illumination, the photocurrent increases in the reverse bias condition, while an insignificant change in current is observed in the forward bias condition [61]. The separation of photogenerated charge carriers in p-n junction device plays a key role in its photodetection efficiency. This can be achieved by the formation of high quality p-n junction and hence strong built-in electric field in the depletion region [187]. As a result, large increase in photocurrent of few-layer MoS_2/Si heterojunction under reverse bias condition has been observed upon illumination, as shown in **Figure 5.3 (c)**. As the bias potential increases the current increases due to increasing driving force for conduction of photogenerated electrons and holes in few-layer MoS_2. Increasing photocurrent with white light intensity in reverse bias can be observed in **Figure 5.3 (c)**, which can be directly attributed to the increased number of photogenerated charge carriers. We also observed the variation of photocurrent with reverse bias voltage, as shown in **Figure 5.3 (d)**, which clearly indicates the linear dependence of photocurrent on reverse bias voltage.

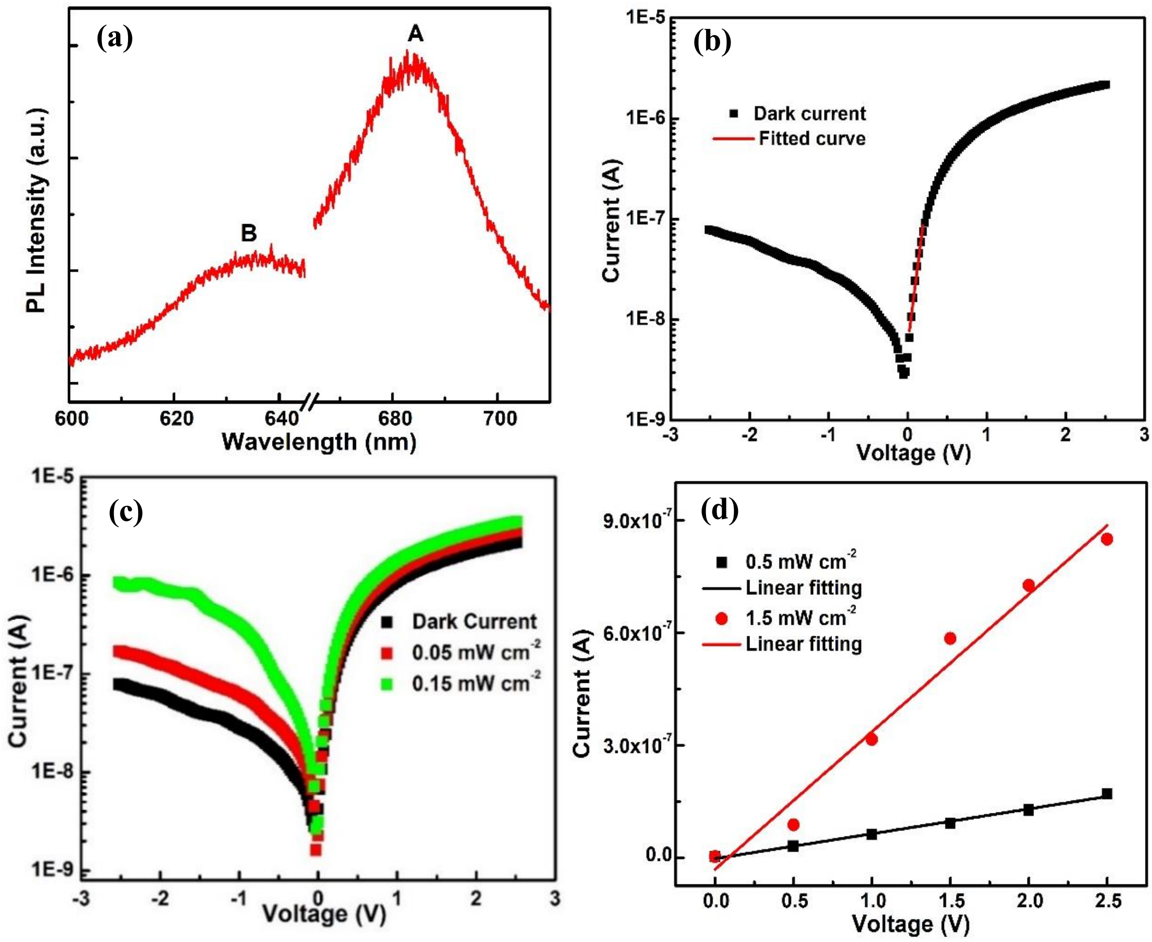

Figure 5.3 *(a) Photoluminescence spectrum of interconnected network of few-layer* MoS_2 *grown over Si substrate (b) Current-Voltage (I-V) characteristics curve of few-layer* MoS_2*/Si heterojunction at dark conditions. (c) Current-Voltage (I-V) curve under dark and white light illumination. (d) Reverse bias current vs reverse bias voltage.*

The choice of a suitable photodetector depends on different factors such as spectral selectivity, photoresponsivity, speed and sensitivity towards low light detection. Standard terminology and figures of merit are crucial for describing and comparing different photodetectors. In order to determine the efficiency of few-layers MoS_2/Si heterojunction photodiode, we have calculated its photoresponsivity (R), which describes how a photodetector system responds to the light illumination. It is defined as output photocurrent per unit incoming optical power of the illumination source per unit active area of the photodetector and is given by following **equation 5.2** -

$$R = \frac{I_{ph}}{P_{inc}S} \tag{5.2}$$

where P_{inc} is the incident power intensity of illuminated source falling normally on sample, I_{ph} represents photocurrent and S is the illuminated area of the few-layer MoS_2 [96]. The maximum responsivity of 0.1413 A W^{-1} under white light of power 0.15 mW cm^{-2} at -2 V is found for few-layer MoS_2/Si heterojunction photodiode. The conduction mechanisms of few-layer MoS_2/Si heterojunction can be explained on the basis of energy band diagrams, as shown schematically in **Figure 5.4**. Different materials have different work functions and Fermi levels. The fermi level of a p-type material is located close to the valence band edge and fermi level of a n-type material is located close to conduction band edge, as shown in **Figure 5.4 (a)** and their relative positions depend upon the concentration of the doping. In general, the electron flow from the higher fermi energy level (n-type MoS_2) to the lower fermi energy level (p-type Si) and an electric field is developed from n-MoS_2 to p-Si at the junction, when two semiconductors are in contact with each other without any bias. The band bends up in the direction of the electric field. When two different type of materials come in contact, band structure evolves due to the alignment of the Fermi levels. In equilibrium condition, the conduction (E_C) and the valence (E_V) bands bend down in p-type material at junction, while E_C and E_V of n-type materials bend up resulting in formation of energy barrier. The alignment of the E_C and the E_V bands of p-type Si and n-type few-layer MoS_2 in equilibrium on contact is shown in **Figure 5.4 (b)**. **Figure 5.4 (c)** shows the band alignment in forward bias condition and **Figure 5.4 (d)** indicates the band alignment in reverse bias condition of n-MoS_2/p-Si heterojunction. The levels in band diagram have been chosen as per literature reports [61, 95, 185, 192, 193]. At zero bias, movement of charge carriers in a few-layer MoS_2 and Si is restricted due to the presence of depletion layer at p-n junction resulting in insignificant current.

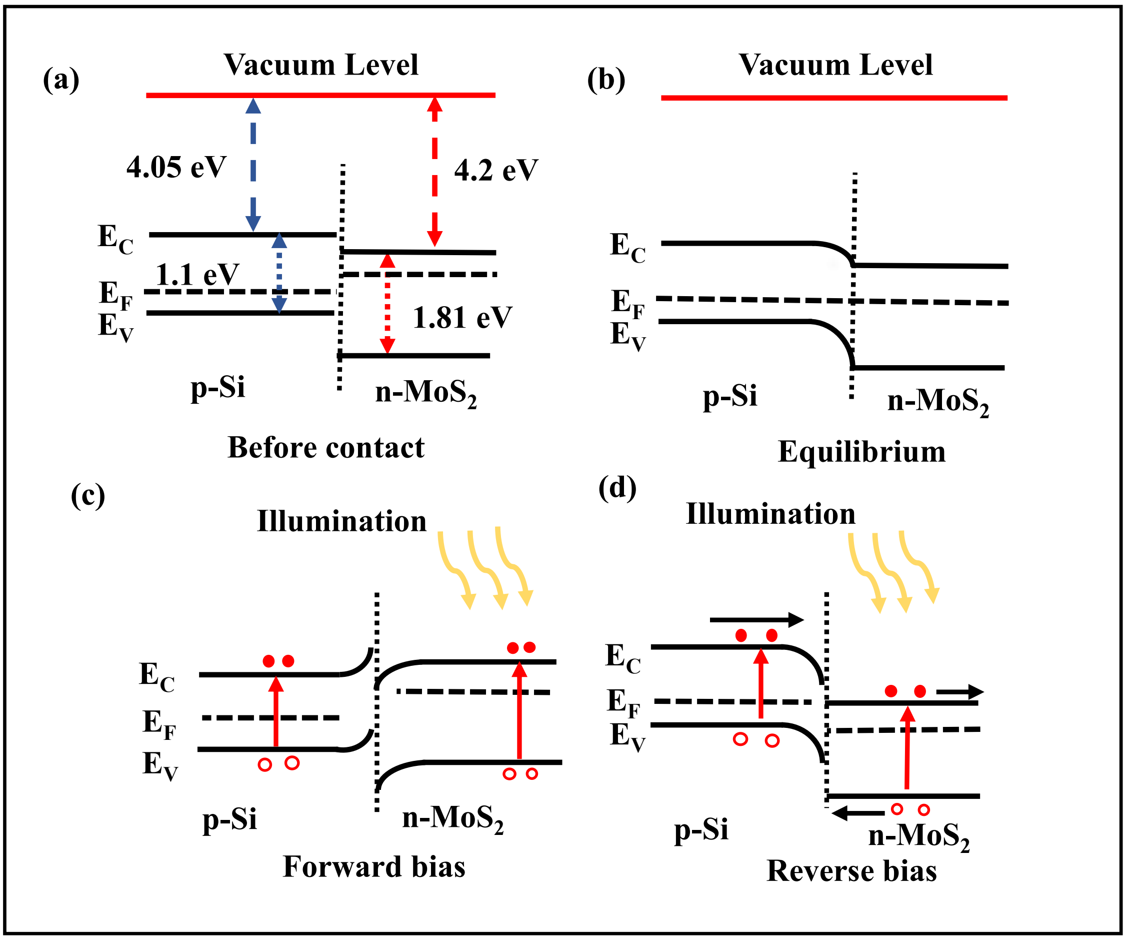

Figure 5.4 *Schematic band diagram of p-type Si and n-MoS_2 (a) Before contact (b) equilibrium (c) Forward bias and (d) Reverse bias conditions. E_C, E_V, and E_F denote the conduction band, valence band, and Fermi energy level, respectively.*

In the forward bias condition, the photogenerated charge carriers in the few-layer MoS_2 cannot move to the Si, due to the upward bending of bands in p-type Si and downward bending of bands in n-type MoS_2. The recombination of charge carriers take place and hence insignificant change in photocurrent is observed upon illumination [185, 193, 194]. At reverse bias, the band bending results in an increase in the depletion layer. The photogenerated electron-hole pairs are then separated by built-in electric field of the depletion region and are collected by electrodes to result in a significant change in photocurrent under reverse bias condition upon illumination [61].

5.2.2 Photodetection Behaviour of Vertically Oriented Few-Layer MoS_2

In another work, we have successfully synthesized high quality vertically oriented few-layer MoS_2 (VFL-MoS_2) over large area (1x1 cm^2) of p-type Si substrate using CVD method. We have studied their morphology and semiconducting properties for photodetection application. In the following section, we discuss the photodetection performance of VFL- MoS_2 /Si heterojunction in detail.

5.2.2.1 Characterization of Vertically Oriented Few-Layer MoS_2

The photograph of V-type MoS_2 grown over 1×1 cm^2 area of Si substrate is shown in **Figure 5.5 (a)**. The optical contrast of the growth region indicates the centimetre scale growth. Surface morphology of the VFL-MoS_2 film has been characterized by scanning electron microscopy (SEM). The SEM image of VFL-MoS_2 is shown in **Figure 5.5 (b),** indicating the interconnected vertically oriented MoS_2 over Si substrate. To find the layer number and the crystalline nature of the synthesized film, we performed the transmission electron microscopy (TEM) study. The TEM image of VFL-MoS_2 is shown in **Figure 5.5 (c)**, indicating thin layer of MoS_2 with thickness around 5 nm and presence of six to seven layers. **Figure 5.5 (d)** shows the selective area electron diffraction (SAED) pattern for VFL-MoS_2, displaying sets of hexagonal symmetrical patterns, indicating the hexagonal lattice structure of MoS_2 crystal [37]. The crystalline nature of VFL-MoS_2 is further confirmed by X-ray diffraction (XRD) study. **Figure 5.5 (e)** shows the XRD peaks of VFL-MoS_2 at 2θ = 14.06°, 28.75°, 43.97°, and 60.02°, corresponding to (002), (004), (006) and (008) for MoS_2 (JCPDS card No. 37-1492), respectively. The XRD pattern suggests the hexagonal symmetric (2H) phase of VFL-MoS_2 and orientation of individual MoS_2 nanosheets in [001] direction, as reported in the literature for 2D materials with a vertical orientation [96, 159].

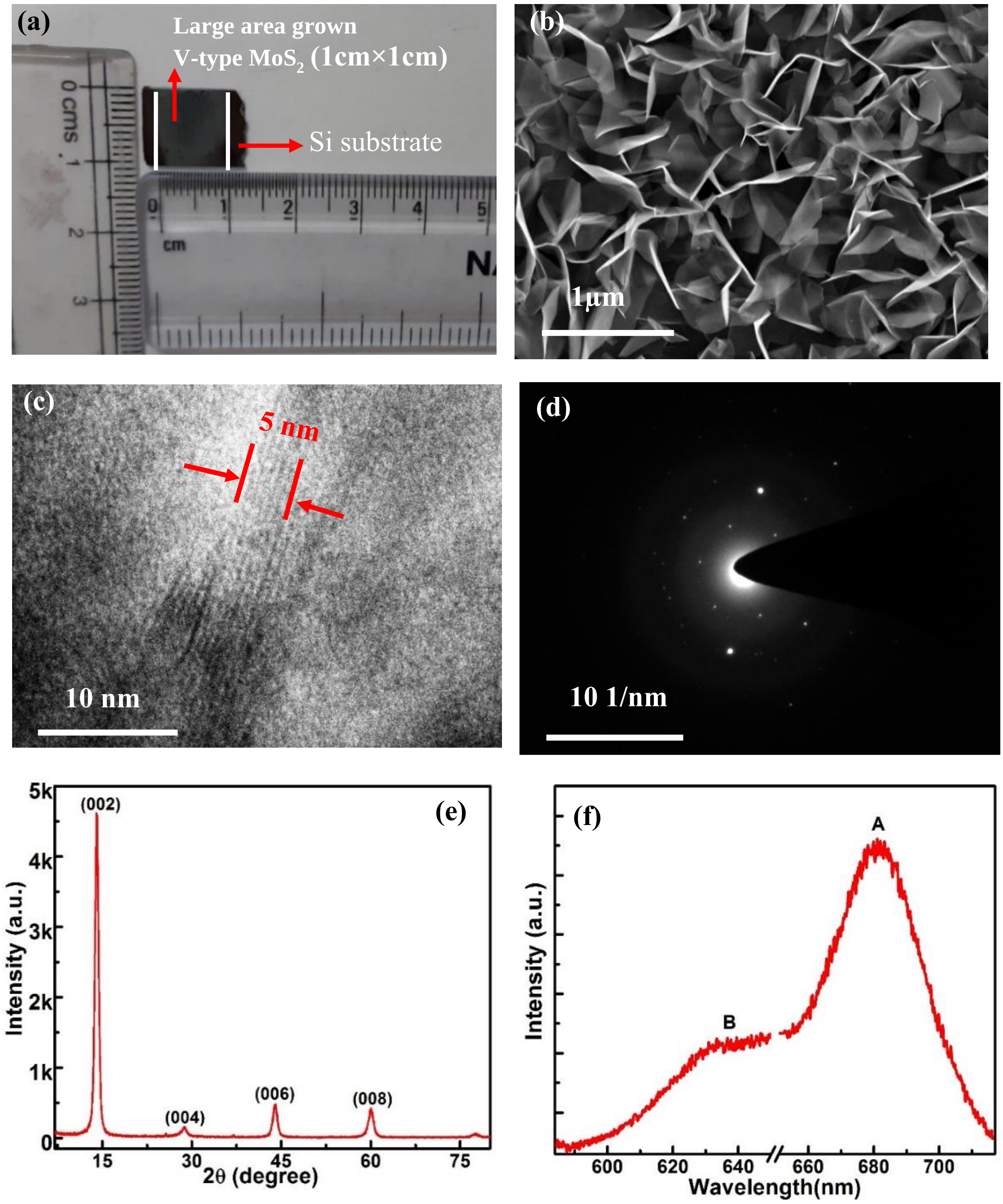

***Figure 5.5** (a) Photograph of VFL-MoS_2 grown over Si indicating 1x1 cm^2 growth region, (b) SEM image, (c) HRTEM image, (d) SAED pattern, (e) XRD pattern and (f) Photoluminescence spectrum of VFL-MoS_2 grown over Si substrate.*

The 2H-phase of VFL-MoS_2 has also been confirmed by Raman spectroscopy technique, which has been already discussed in detail in **Figure 3.6 (f)** of **Chapter 3**. The semiconducting behavior of VFL-MoS_2 has been examined by photoluminescence (PL) study. The PL spectrum, shown in **Figure 5.5 (f)**, indicates a higher intensity peak around

681 nm for direct A excitons (~ 1.82 eV) and relatively lower intensity hump around 635 nm for B excitons (~ 1.95 eV), as reported in literature [167]. These two excitons are generated due to the spin-orbit coupling at the K-point of the valence band. At room temperature, we observe the good PL intensity in VFL-MoS_2, indicating its possible use in photodetection application.

5.2.2.2 Photoresponse of Vertically Oriented Few-Layer MoS_2/Si Heterojunction

We have also directly grown vertically oriented few layer (VFL)-MoS_2 (n-type) over p-type Si substrate using CVD technique to form heterojunction and used as a photodiode under 532 nm illumination at different excitation laser powers. The I-V characteristics of VFL-MoS_2/Si heterojunction exhibits rectifying behaviour in the dark condition, as shown in **Figure 5.6 (a)**. The high degree of asymmetry in dark current suggests the formation of good quality p-n junction at VFL-MoS_2/Si interface. We observe the ideality factor (η)~ 2.58 for this heterojunction from the dark current using **equation 5.1**. The ideality factor is expected to have value between 1 and 4. The deviation of ideality factor from ideal value 1 in the present case can be attributed to the possible electron-hole recombination due to surface states at the heterostructure interface. The I-V characteristics of VFL-MoS_2/Si heterojunction at different laser power intensity is shown in **Figure 5.6 (b)**. Moreover, it is observed that the reverse-biased current increases with illumination intensity due to enhanced photogenerated charge carriers. The excellent p-n junction formation at VFL-MoS_2/Si interface leads to the efficient separation of photogenerated charge carriers (electrons and holes) under reverse bias due to the built-in electric field in the depletion region [24, 95, 194]. The figure-of-merit parameter, photoresponsivity (R) indicates the photodetection efficiency and is calculated using **equation 5.2**. The calculated photoresponsivity of VFL-MoS_2/Si heterojunction is found to be around 7.37 A W^{-1} under the illumination laser power of 0.15 mW cm^{-2} at –2

V. The obtained photoresponsivity of our device is found to be better than other reports on MoS_2/Si heterojunction, as summarized in **Table-5.1**. This high photoresponsivity of our device can be ascribed to the strong light absorption due to multiple reflection of light in interconnected network of vertical MoS_2, intralayer carrier transport speed and efficient electron-hole separation at VFL-MoS_2/Si interface [96].

The photocurrent of our fabricated heterojunction device shows a strong dependence on the laser power density at reverse bias. The relationship between the photocurrent and the laser power density is well explained by the power law. The reverse biased photocurrent depends on laser power density as follows [195] -

$$I_{ph} = C\mathrm{P}_{inc}^{\alpha} \tag{5.3}$$

where C is a scaling constant and α is the exponent parameter related to the response of the photocurrent to the light intensity. This law gives an idea about the variation of the photocurrent with respect to the incident illumination intensity. The exponent parameter (α) value close to ideal value i.e. 1, represents the low trap states at junctions of the device. However, its value less than 1 represents the possibility of carrier generation, recombination, defects, or trapping inside the device. The calculated α value for our device is found to be around 0.92, as shown in **Figure 5.6 (c)**, indicating low photocurrent loss for the present device. This may be attributed to the possibility of lower recombination and trapping of charge carriers in our device [94]. **Figure 5.6 (d)** shows the switching ability of VFL-MoS_2/Si photodiode at laser power of 5.15 mW cm^{-2} and applied voltage -3V, clearly indicating the excellent photoresponse with time under periodic switching ON/OFF of laser. The steep rise and fall with respect to light on and off in our heterojunction device suggest a fast response speed, showing that charge carriers are effectively generated and separated in the VFL-MoS_2/Si photodiode. The excellent optoelectronic behaviour of VFL-MoS_2 can be attributed to the high aspect ratio, highly exposed edges and increased light trapping by multiple reflection [94, 96]. The conduction mechanism of VFL-MoS_2/Si heterojunction is similar to the few-layer MoS_2 /Si heterojunction photodiode as shown in **Figure 5.4**.

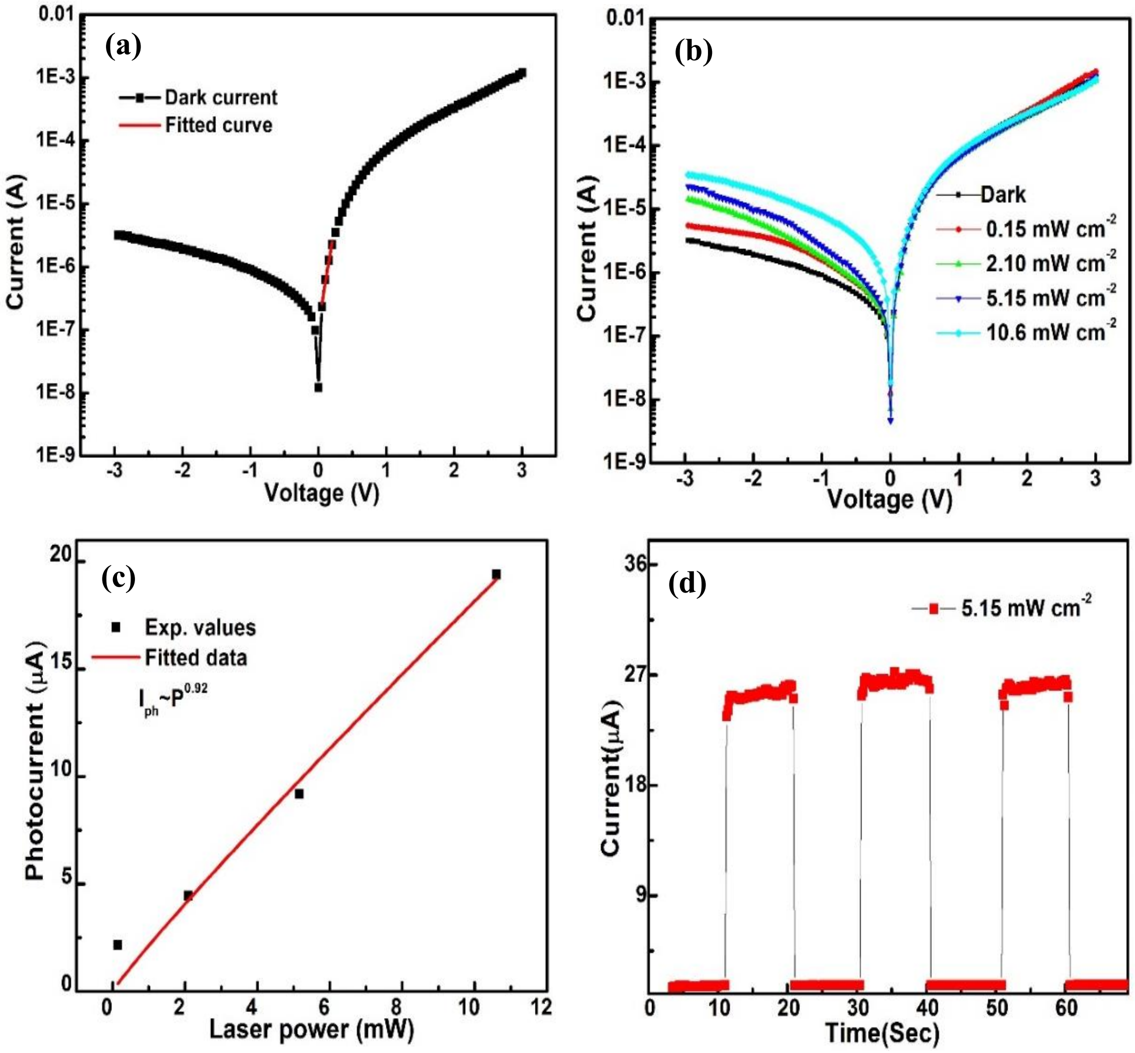

Figure 5.6 *(a) I-V characteristics of VFL-MoS_2/Si p-n junction photodiode under dark condition. (b) I-V curves of VFL-MoS_2/Si photodiode under dark and different illumination. (c) Photocurrent vs laser intensities at -2V. (d) Switching behaviour of photodiode at -3V.*

Table 5.1 Comparison of Responsivity of MoS_2/Si Heterojunction Photodiodes.

Photodiode junction (synthesis method)	**Light source (wavelength)**	**Intensity (mW cm^{-2})**	**Bias potential (V)**	**Responsivity (A W^{-1})**	**Reference**
Few-layer MoS_2/Si (CVD)	White light	0.15	-2 V	0.1413	**Present work**
Few-layer vertically oriented MoS_2/Si (CVD)	Laser (532 nm)	0.15	-2 V	7.37	**Present work**
Few-layer MoS_2/Si (Solution process)	Laser (514 nm)	3	-2V	0.045	J. Mater. Chem. A, 2016, **4**, 4534−4543.[24]
Multi-layer MoS_2/Si (CVD)	- (514 nm)	-	3V	8.75	Sci. Rep., 2017, **7**, 44243−44252.[61]
Few-layer V-type MoS_2/Si (CVD)	Laser (808 nm)	1.6	-2V	0.908	J. Mater. Chem. C, 2018, **6**, 3233−3239.[96]
Few-layer V-type MoS_2/Si (Sputtering)	Laser (808 nm)	1	-	0.3	Adv. Funct. Mater., 2015, **25**, 2910−2919.[189]
MoS_2 quantum dot/Si (Sono-chemical process)	Laser (514 nm)	-	-2V	2.8	Sci. Rep., 2016, **6**, 29016−29027.[95]
MoS_2 nanocrystal/Si (Solution process)	Laser (514 nm)	0.2×10^{-3}	-2V	0.47	Nanotechnology, 2017, **28**, 135203−135214.[97]

5.3 Conclusions

In this chapter, we have demonstrated the photodetection application of interconnected network of horizontally grown few-layer MoS_2 over Si for low-power white light detection and showed its photoresponsivity of 0.1413 A W^{-1} under low-power white light (~0.15 mW cm^{-2}) illumination at −2 V. The good responsivity can be associated to the formation of a good quality p-n junction and effective separation of charge carriers. Further, we have successfully demonstrated the VFL-MoS_2 based p-n junction photodetector for detection of green light of wavelength 532 nm. We have found excellent photodetection with responsivity around 7.37 A W^{-1} at −2 V bias under a laser intensity of 0.15 mW cm^{-2}. The high photoresponsivity and excellent optoelectronic behaviour of VFL-MoS_2 can be attributed to the high aspect ratio, highly exposed edges and increased light trapping by multiple reflection of light. These studies clearly suggest that few-layer MoS_2 can be used for photodetection purposes. These MoS_2 nanostructures based photodetectors can be used in sensors, night vision devices, surveillance, optical communications etc.